atmosphere

MDPI

Article

Analysis of Carbon Source/Sink Driving Factors Under Climate Change in the Inner Mongolia Grassland Ecosystem Through MGWR

Ritu Wu [1,2], Zhimin Hong [2], Wala Du [1,3,*], Hong Ying [4], Rihan Wu [4], Yu Shan [4,5], Sainbuyan Bayarsaikhan [6,7] and Dan Xiang [2]

[1] Institute of Grassland Research, Chinese Academy of Agricultural Sciences, Hohhot 010022, China; 20221100075@imut.edu.cn
[2] College of Science, Inner Mongolia University of Technology, Hohhot 010051, China; zhmhong@imut.edu.cn (Z.H.); 20221100076@imut.edu.cn (D.X.)
[3] Arshan Forest and Grassland Disaster Prevention and Mitigation Field Scientific Observation and Research Station of Inner Mongolia Autonomous Region, Arshan 137400, China
[4] College of Geographic Science, Inner Mongolia Normal University, Hohhot 010022, China; hongy864@nenu.edu.cn (H.Y.); wurh651@imnu.edu.cn (R.W.); yushan@imnu.edu.cn (Y.S.)
[5] Inner Mongolia Key Laboratory for Resource-Environmental Information System, Hohhot 010051, China
[6] Department of Geography, School of Arts and Sciences, National University of Mongolia, Ulaanbaatar 14200, Mongolia; sainbuyan.b@num.edu.mn
[7] Laboratory of Geo-Informatics (GEO-iLAB), Graduate School, National University of Mongolia, Ulaanbaatar 14200, Mongolia
* Correspondence: duwala@caas.cn

Abstract: Grassland ecosystems are essential components of the global ecosystem. They may efficiently reduce CO_2 concentrations in the atmosphere and play a vital role in mitigating climate change. The objectives of this study were to reveal the spatial distribution features of net primary production (NPP) and net ecosystem productivity (NEP) under climate change in the Inner Mongolia grassland ecosystem, China, and to devise effective management strategies for grassland ecosystems. Based on the multiscale geographically weighted regression (MGWR) model, this study investigated the spatial variation features of NPP and NEP along with their driving factors. The results showed the following: (1) The annual average NPP in the Inner Mongolia grassland ecosystem was 234.22 $gC \cdot m^{-2} \cdot a^{-1}$, and the annual average NEP was 60.31 $gC \cdot m^{-2} \cdot a^{-1}$ from 2011 to 2022. Both measures showed a spatial pattern of high values in the northeast and low values in the southwest, as well as a temporal pattern of high values in summer and low values in winter. (2) The normalized difference vegetation index (NDVI) and solar radiation had promoting effects on NPP, where NDVI had the largest significant positive correlation area. In addition, precipitation and temperature on the influence of NPP were significantly negative with a larger area. (3) The area with a significant positive correlation of NDVI, solar radiation, and precipitation on NEP was larger than that with a significant negative correlation, while the area with significant negative correlation of temperature was larger. This study used the MGWR model to explore the relationship between NPP, NEP, and multiple factors. The results showed regional variation in NPP and NEP under the combined effect of various drivers. This contributes to a better understanding of carbon sinks under climate change in the Inner Mongolia grassland ecosystem.

Keywords: grassland ecosystem; net primary production; net ecosystem productivity; multiscale geographically weighted regression; climate change

check for updates

Academic Editor: Gareth Marshall

Received: 13 March 2025
Revised: 29 April 2025
Accepted: 12 May 2025
Published: 16 May 2025

Citation: Wu, R.; Hong, Z.; Du, W.; Ying, H.; Wu, R.; Shan, Y.; Bayarsaikhan, S.; Xiang, D. Analysis of Carbon Source/Sink Driving Factors Under Climate Change in the Inner Mongolia Grassland Ecosystem Through MGWR. *Atmosphere* **2025**, *16*, 607. https://doi.org/10.3390/atmos16050607

Copyright: © 2025 by the authors. Licensee MDPI, Basel, Switzerland. This article is an open access article distributed under the terms and conditions of the Creative Commons Attribution (CC BY) license (https://creativecommons.org/licenses/by/4.0/).

1. Introduction

Carbon dioxide (CO_2) is one of the main factors contributing to the progressive warming of the global climate [1]. China has set targets of attaining a "carbon emissions peak" by 2030 and "carbon neutrality" by 2060 to reduce global warming and promote sustainable growth. To achieve carbon neutrality, emissions must be reduced and carbon sinks must be improved [2]. In general, an ecosystem is considered a carbon sink when it absorbs more carbon than it emits; otherwise, it is a carbon source [3]. Grassland ecosystems are essential components of the global ecosystem, since they may efficiently reduce CO_2 concentrations in the atmosphere and play a vital role in mitigating climate change [4–6]. Inner Mongolia has the largest grassland vegetation carbon pool in China [7], making it one of the most vulnerable regions to global climate change. Therefore, studying the relationship between carbon sources/sinks and driving factors in the Inner Mongolian grassland ecosystem is critical to understanding global climate change [8].

Net primary productivity (NPP) reflects the ability of vegetation to fix atmospheric CO_2 through photosynthesis and can thus be used to reflect the carbon cycle in an ecosystem. NPP is also the primary factor determining ecosystem carbon sources/sinks, and thus cannot be overlooked when aiming for "carbon neutrality" [3]. Net ecosystem productivity (NEP) is the difference between photosynthesis and respiration in an ecosystem and is also the difference between the amount of carbon absorbed by the NPP of plants and the amount of carbon exhaled by soil heterotrophic respiration (R_h) [3,9,10]. Therefore, NEP can indicate whether an ecosystem acts as a carbon source or sink, reflecting its carbon sequestration capacity [3].

In ecology, net ecosystem exchange (NEE) is used to quantify the exchange of CO_2 between terrestrial ecosystems and the atmosphere. It reflects whether the ecosystem absorbs or releases CO_2 within a certain period of time. NEP and NEE are numerically similar but have opposite signs. Both are important indicators for describing the carbon cycle in ecosystems. NEP is closely related to soil carbon accumulation and can more stably reflect the long-term carbon sequestration capacity of the ecosystem [11].

Currently, there is much research on estimation methods for NPP and NEP [9,12,13]. The three main methods for estimating NPP are light energy utilization models, terrestrial ecosystem process models [14], and climate productivity models [15]. The Carnegie Ames Stanford approach (CASA) model, based on light energy utilization, is widely used by scholars due to its simplicity and practicability for calculating NPP. It uses factors such as NDVI, solar radiation, temperature, and precipitation to calculate NPP. This method is suitable for regional NPP calculation and shows little difference between the estimated and measured NPP [13]. Liang et al. used this model to calculate China's NPP, while Yin et al. used it to calculate the NPP of the Mongolian Plateau. Both studies proved that the model's simulated results closely resemble actual satellite data when used correctly [13,16]. Based on this model, NEP is defined as the difference between NPP and R_h. Thus, only the value of R_h must be determined to obtain the value of NEP [17]. R_h can be calculated by establishing an empirical equation between the environmental factors and R_h [18]. This formula has been widely applied in various regions of China since it was proposed by Pei et al. in 2009 [18]. For example, K. Zhang et al. calculated the R_h in the Yellow River Basin, and Zhang et al. calculated the R_h in arid Central Asia, demonstrating that the formula performed well in each region [12,19].

To date, some findings have been obtained to characterize the spatiotemporal distribution of NPP and NEP, and to analyze the factors influencing them [8,20–26]. Some studies have used correlation and regression analyses to investigate the influence of driving factors on NPP and NEP. Dai et al. studied spatiotemporal features of carbon source/sink and their relationship with climate factors in the Inner Mongolia grassland ecosystem [8].

Li et al. and Xu et al. used correlation analysis to explore the response of NPP and NEP to temperature, precipitation, and solar radiation [20,23]. Ge et al. used residual analysis to study the influence of meteorological factors on NPP [22]. They discovered variations in the impact of driving factors on NPP and NEP across different regions and types of vegetation. From the above studies, it is evident that there is spatial variation in the effect of each driving factor on NPP and NEP. Liu et al. and Zhang et al. used the geographically weighted regression (GWR) model and the geographical and temporal weighted regression (GTWR) model, respectively, to investigate spatial heterogeneity and spatiotemporal heterogeneity in the impacts of the driving factors on NPP and NEP [24,25]. However, the heterogeneous relationships are based on uniform temporal and spatial scales. This approach of "averaging" the scales of all the explanatory variables may neglect the scale-effect problem of the different explanatory variables. Since different explanatory variables have varying spatial effects on the response variable, a separate bandwidth needs to be given for each explanatory variable. This means that each explanatory variable requires its own separate bandwidth.

To address this issue, Fotheringham et al. proposed a multiscale geographically weighted regression (MGWR) model. This model determines a separate spatial bandwidth for each explanatory variable, reflecting the scale effect of the impact of different explanatory variables. Since then, the model has been implemented in various fields and has shown improved results [1,27–31]. Xu et al. used the MGWR model to investigate the spatial heterogeneity of the factors influencing carbon emission intensity in the China Yangtze River Delta region, while Shen et al. and Lu et al. used it to address the problem of housing prices, thus showing that the model's application in different fields has achieved good results [1,27,28].

Based on meteorological data, solar radiation data, and vegetation cover data from satellite remote sensing, we first calculated the NPP and NEP in Inner Mongolia grassland ecosystems with the CASA model and the soil microbial respiration model. Second, we fitted the driving factors to the NPP and NEP through the MGWR model from 2011 to 2022 and analyzed how climate change, vegetation factors, and solar radiation have impacted the spatial change characteristics of the NPP and NEP in the Inner Mongolia grassland ecosystem. The study's findings are crucial for scientific knowledge and for improving the effective management of grassland ecosystems.

2. Materials and Methods

2.1. Study Area

Inner Mongolia ($37^{\circ}24'$–$53^{\circ}23'$N, $97^{\circ}12'$–$126^{\circ}04'$E) is located in northern China (Figure 1), with a total area of approximately 118.3×10^4 km^2 and a straight east–west span of nearly 2400 km. Within this area, 786,000 km^2 is natural grassland, accounting for 66.4% of the total area [32]. The majority of Inner Mongolia has a typical temperate continental monsoon climate. The average annual temperature ranges from 3 to 6 °C, increasing from northeast to southwest. The total annual solar radiation ranges from 0.5 to 0.7 MJ $\cdot$ cm^{-2}, also increasing from east to west, and the average annual precipitation ranges from 100 to 400 mm, decreasing from northeast to southwest [8,32,33].

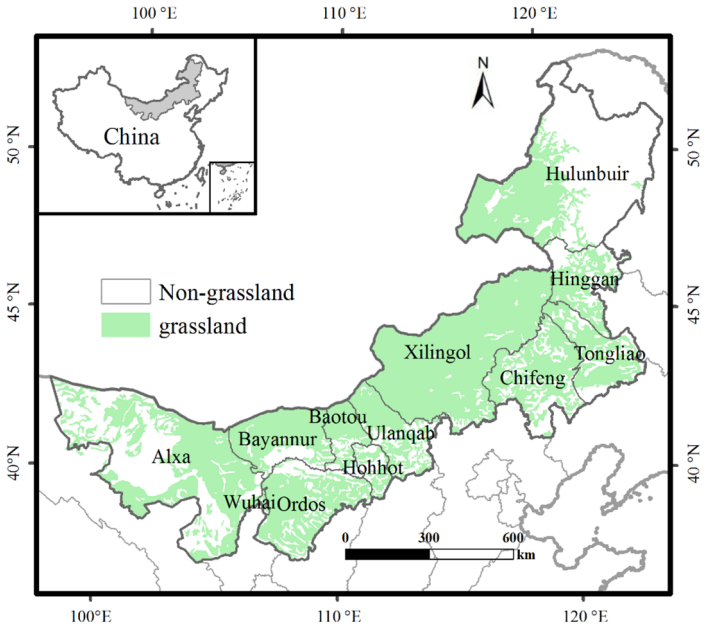


Figure 1. Location of study area.

2.2. Materials

MODIS NDVI came from the National Aeronautics and Space Administration (NASA) MOD13A3 product via the Terra satellite platform "https://doi.org/10.5067/MODIS/MOD13A3.006 accessed on 19 June 2024)", with spatial and temporal resolutions of 1 km and 1 month, respectively. To obtain the required data, the MODIS reprojection tool (MRT) was used, and batch processing (such as mosaic and projection conversion) was performed. Meteorological data (monthly average temperature and monthly total precipitation) and solar radiation data came from the European Centre for Medium-Range Weather Forecasts Reanalysis v5 (ECMWF ERA5) climate reanalysis dataset "https://cds.climate.copernicus.eu/datasets/reanalysis-era5-single-levels-monthly-means?tab=overview (accessed on 19 June 2024)", and the surface downward solar radiation of ERA5 monthly data were used as the solar radiation data from 2011 to 2022 [34]. Description of the data above is listed as Table 1. Because the datasets had different spatial resolutions, a resampling technique was used to change the spatial resolution of the MODIS NDVI data to 0.1° × 0.1°. This step was intended to ensure that the data were spatially aligned for subsequent analysis.

Table 1. Description of data used in this study.

Name	Description	Resolution
NDVI	Developed from NASA MOD13A3 "https://doi.org/10.5067/MODIS/MOD13A3.006 (accessed on 19 June 2024)"	1 km
Temperature	Developed from ECMWF ERA5 "https://cds.climate.copernicus.eu/datasets/reanalysis-era5-single-levels-monthly-means?tab=overview (accessed on 19 June 2024)"	0.1° × 0.1°
Precipitation	Developed from ECMWF ERA5 "https://cds.climate.copernicus.eu/datasets/reanalysis-era5-single-levels-monthly-means?tab=overview (accessed on 19 June 2024)"	0.1° × 0.1°
Solar radiation	Developed from ECMWF ERA5 "https://cds.climate.copernicus.eu/datasets/reanalysis-era5-single-levels-monthly-means?tab=overview (accessed on 19 June 2024)"	0.1° × 0.1°

Abbreviations: NDVI = monthly normalized difference vegetation index, Temperature = monthly average temperature, Precipitation = monthly total precipitation, Solar radiation = monthly total solar radiation.

2.3. Research Methods

2.3.1. Estimation of NPP

The NPP based on the CASA model was calculated using the following formula [35]:

$$\mathrm{NPP}(x,t) = \mathrm{APAR}(x,t) \times \varepsilon(x,t) \tag{1}$$

where $\mathrm{APAR}(x,t)$ is the photosynthetically active radiation absorbed by pixel x at time $t\left(\mathrm{gC}\cdot\mathrm{m}^{-2}\cdot\mathrm{month}^{-1}\right)$, $\varepsilon(x,t)$ is the actual light energy utilization of pixel x at time $t\left(\mathrm{gC}\cdot\mathrm{MJ}^{-1}\right)$, and the expressions for $\mathrm{APAR}(x,t)$ and $\varepsilon(x,t)$ are calculated as follows:

$$\mathrm{APAR}(x,t) = \mathrm{SOL}(x,t) \times \mathrm{FPAR}(x,t) \times 0.5 \tag{2}$$

where $\mathrm{SOL}(x,t)$ is the total solar radiation of pixel x at time $t(\mathrm{MJ}\cdot\mathrm{m}^{-2}\cdot\mathrm{month}^{-1})$ and $\mathrm{FPAR}(x,t)$ is the proportion of incident photosynthetically active radiation absorbed by the vegetation layer. 0.5 denotes the proportion of total solar radiation utilized by vegetation.

$$\mathrm{FPAR}(x,t) = \alpha\mathrm{FPAR}_{\mathrm{NDVI}} + (1-\alpha)\mathrm{FPAR}_{\mathrm{SR}} \tag{3}$$

where α = 0.05, and the calculation formulae of $\mathrm{FPAR}_{\mathrm{NDVI}}$ and $\mathrm{FPAR}_{\mathrm{SR}}$ are as follows:

$$\mathrm{FPAR}_{\mathrm{NDVI}} = \frac{\mathrm{NDVI}(x,t) - \mathrm{NDVI}_{i,\min}}{\mathrm{NDVI}_{i,\max} - \mathrm{NDVI}_{i,\min}} \times (\mathrm{FPAR}_{\max} - \mathrm{FPAR}_{\min}) + \mathrm{FPAR}_{\min} \tag{4}$$

$$\mathrm{FPAR}_{\mathrm{SR}} = \frac{\mathrm{SR}(x,t) - \mathrm{SR}_{i,\min}}{\mathrm{SR}_{i,\max} - \mathrm{SR}_{i,\min}} \times (\mathrm{FPAR}_{\max} - \mathrm{FPAR}_{\min}) + \mathrm{FPAR}_{\min} \tag{5}$$

$$\mathrm{SR}(x,t) = \frac{1+\mathrm{NDVI}(x,t)}{1-\mathrm{NDVI}(x,t)} \tag{6}$$

where $\mathrm{NDVI}(x,t)$ represents the NDVI value of pixel x at time t, with $\mathrm{NDVI}_{i,\min}$ = 0.023 and $\mathrm{NDVI}_{i,\max}$ = 0.634. Among these, $\mathrm{FPAR}_{\max}$= 0.95 and $\mathrm{FPAR}_{\min}$= 0.001, respectively. SR is the ratio vegetation index; $\mathrm{SR}_{i,\min}$ = 1.05 and $\mathrm{SR}_{i,\max}$ = 4.46.

$$\varepsilon(x,t) = T_{\varepsilon 1}(x,t) \times T_{\varepsilon 2}(x,t) \times W_{\varepsilon}(x,t) \times \varepsilon_{\max} \tag{7}$$

where $T_{\varepsilon 1}(x,t)$ reflects the reduction in NPP due to the limitation of photosynthesis by intrinsic plant biochemistry at low and high temperatures. $T_{\varepsilon 2}(x,t)$ indicates the trend of decreasing light energy utilization by plants as the ambient temperature changes from the optimal temperature to higher or lower temperatures. $W_{\varepsilon}(x,t)$ reflects the effect of moisture on light energy utilization. $\varepsilon_{\max}$ is the maximum light energy utilization under ideal conditions, where $\varepsilon_{\max}$ = $0.542\left(\mathrm{gC}\cdot\mathrm{MJ}^{-1}\right)$.

$$T_{\varepsilon 1}(x,t) = 0.8 + 0.02 \times \mathrm{T}_{\mathrm{opt}}(x) - 0.0005 \times \left[\mathrm{T}_{\mathrm{opt}}(x)\right]^2 \tag{8}$$

where $\mathrm{T}_{\mathrm{opt}}(x)$ is the optimum temperature for plant growth, specifically the average temperature (°C) of the month, when the NDVI value of a certain region reaches its maximum in a year. When the average temperature $\mathrm{T}(x,t)$ in a month is less than or equal to −10 °C, the NDVI value will be 0.

$$\begin{aligned} T_{\varepsilon 2}(x,t) = \; & 1.184/\left\{1+\exp\left[0.2\times\left(\mathrm{T}_{\mathrm{opt}}(x)-10-\mathrm{T}(x,t)\right)\right]\right\} \\ & \times 1/\left\{1+\exp\left[0.3\times\left(-\mathrm{T}_{\mathrm{opt}}(x)-10+\mathrm{T}(x,t)\right)\right]\right\} \end{aligned} \tag{9}$$

when the average temperature $T(x,t)$ in a month is 10 °C higher or 13 °C lower than the optimum temperature $T_{opt}(x)$, the value of $T_{\varepsilon 2}(x,t)$ in a month is equal to half of the $T_{\varepsilon 2}(x,t)$ value when the monthly average temperature $T(x,t)$ is the optimum temperature $T_{opt}(x)$.

$$W_{\varepsilon}(x,t) = 0.5 + 0.5 \times E(x,t)/E_p(x,t) \tag{10}$$

$E(x,t)$ is the actual regional evapotranspiration, and $E_p(x,t)$ is the potential regional evapotranspiration. $E(x,t)$ and $E_p(x,t)$ are calculated as follows [36]:

$$E(x,t) = \frac{P \times R_n \times \left(P^2 + {R_n}^2 + P \times R_n\right)}{(P + R_n) \times \left(P^2 + {R_n}^2\right)} \tag{11}$$

$$R_n = \left(E_p(x,t) \times P\right)^2 \times \left[0.369 + 0.598 \times \left(E_p(x,t)/P\right)^2\right] \tag{12}$$

$$E_p(x,t) = \mathrm{BT} \times 58.93 \tag{13}$$

$$\mathrm{BT} = \frac{1}{12}\sum_{1}^{12} \mathrm{T}_i \tag{14}$$

where P is the precipitation pixel x at time t (mm), R_n is the net solar radiation of pixel x at time t $\left(\mathrm{MJ} \cdot \mathrm{m}^{-2} \cdot \mathrm{month}^{-1}\right)$, BT is the biological temperature, and $\mathrm{T_i}$ is the monthly average temperature of more than 0 °C.

2.3.2. Estimation of NEP

NEP, as a measure of the carbon sink, can be defined as the difference between NPP and $\mathrm{R_h}$ without integrating the effects of human activities [18], as follows:

$$\mathrm{NEP}(x,t) = \mathrm{NPP}(x,t) - \mathrm{R_h}(x,t) \tag{15}$$

$$\mathrm{R_h}(x,t) = 0.22 \times (\exp(0.0912T(x,t) + \ln(0.3145P(x,t) + 1) \times 30 \times 46.5\% \tag{16}$$

where $\mathrm{R_h}(x,t)$ denotes the soil microbial respiration of pixel x at time t $\left(\mathrm{gC} \cdot \mathrm{m}^{-2}\right)$, $T(x,t)$ is the average temperature of pixel x at time t(°C), and $P(x,t)$ is the total precipitation of pixel x at time t(mm).

2.3.3. Multiscale Geographically Weighted Regression Method

Fotheringham et al. proposed the MGWR model in 2017. This allows the regression model to have different spatial scales for the effect of each explanatory variable on the explained variables, providing more comprehensive information. The model can be expressed as follows [31]:

$$y_i = \sum_{j=0}^{p} \beta_{bwj}(u_i, v_i) x_{ij} + \varepsilon_i, i = 1, 2, \ldots, n \tag{17}$$

where bwj is the bandwidth corresponding to the jth covariate, x_{ij} is the observed value of the jth covariate at regression point i, ε_i is the error term and has the assumption of zero mean and homoskedasticity, and $\beta_{bwj}(u_i, v_i)$ is the parameter to be estimated, which can be obtained by using the weighted least squares method:

$$\hat{\beta}_{bwj}(u_i, v_i) = \left[X^T W(u_i, v_i) X\right]^{-1} X^T W(u_i, v_i) Y \tag{18}$$

where $X = [X_0, X_1, \ldots, X_P]$ is the design matrix consisting of the observations of the covariates, X_0 denotes the vector with all components 1, $Y = (y_1, y_2, \ldots, y_n)^T$ represents the observations of the dependent variable, and $W(u_i, v_i) = diag(w_{i1}, \ldots, w_{in})_{n \times n} (i =$

$1, 2, \ldots, n$) is the weight matrix beyond the regression points, usually defined by a Gaussian kernel function or a double square kernel (bi − square) function in the following form:

$$w_{ij} = \begin{cases} [1 - (\frac{d_{ij}}{b_w})^2]^2 & if\ d_{ij} < b_w, \\ 0 & otherwise. \end{cases} \quad (19)$$

where d_{ij} is the distance between regression point i and observation point j, and b_w is the bandwidth. The MGWR model uses the back-fitting algorithm to obtain the bandwidth of each explanatory variable [31].

3. Results

3.1. Spatial Characteristics of NPP and NEP over the Inner Mongolia Grassland Ecosystem

The average NPP of the Inner Mongolia grassland ecosystem was 234.22 gC · m^{-2} · a^{-1} from 2011 to 2022, with obvious regional characteristics, as shown in Figure 2a. The study area showed a spatial pattern of higher NPP in the northeast and lower NPP in the southwest. The highest NPP value was found in northeastern Inner Mongolia. The NPP in central Inner Mongolia was at a moderate level, while the average NPPs in southwestern Inner Mongolia were the lowest. As shown in Figure 2b, the spatial distribution of NEP in the Inner Mongolia grassland ecosystem from 2011 to 2022 showed a spatial pattern of being higher in northeastern Inner Mongolia and lower in southwestern Inner Mongolia. The average NEP of grassland was approximately 60.31 gC · m^{-2} · a^{-1}, indicating that the Inner Mongolia grassland ecosystem was generally classified as a carbon sink (NEP > 0) from 2011 to 2022.

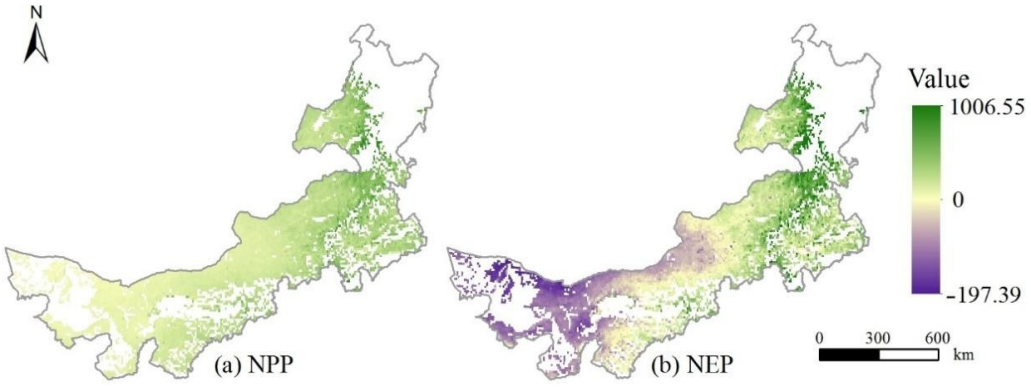


Figure 2. Distribution of NPP (**a**) and NEP (**b**) in the Inner Mongolia grassland ecosystem from 2011 to 2022.

The average area of carbon sources (NEP < 0) from 2011 to 2022 was approximately 322,400 km^2, accounting for 41.02% of the total area of grassland, and the area of carbon sinks was approximately 463,500 km^2, accounting for 58.98% of the total area of grassland (Figure 2b). The grassland carbon sink sectors of Inner Mongolia were located mainly in Hulun Buir, Hinggan, and the eastern part of Xilingol, while the carbon source sectors were located mainly in Alax, Bayannur, and the northern part of Ulanqab. Comparing the carbon sink area with the NPP distribution map (Figure 2a), we concluded that the larger the NPP, the more likely the region is to be a carbon sink area. Conversely, the smaller the NPP, the more likely the region is to be a carbon source region.

There are obvious interannual differences in NPP and NEP in the northern part of Xilingol and the western part of Hulun Buir, as shown in Figures 3 and 4. Moreover, the NPP and NEP in these regions did not simply increase or decrease. Meanwhile, the

remaining regions remained almost unchanged in each year. They retained the spatial characteristics of the entire 12 years from 2011 to 2022.

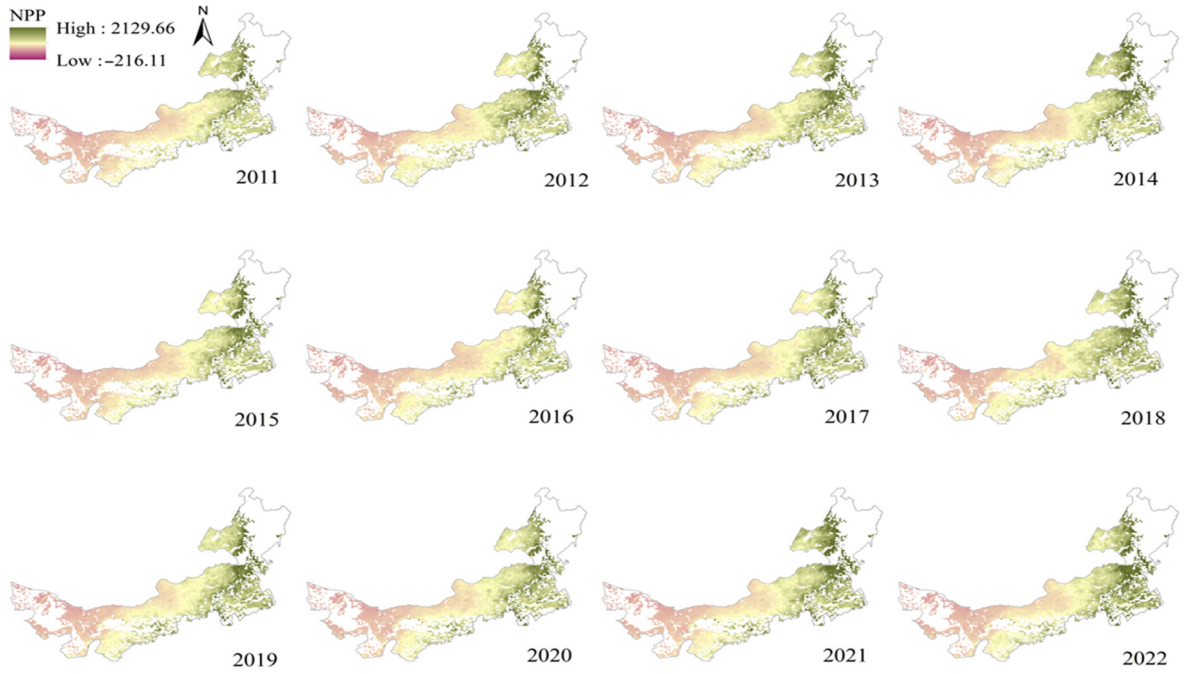


Figure 3. Spatial distribution of the annual average of monthly NPP from 2011 to 2022.

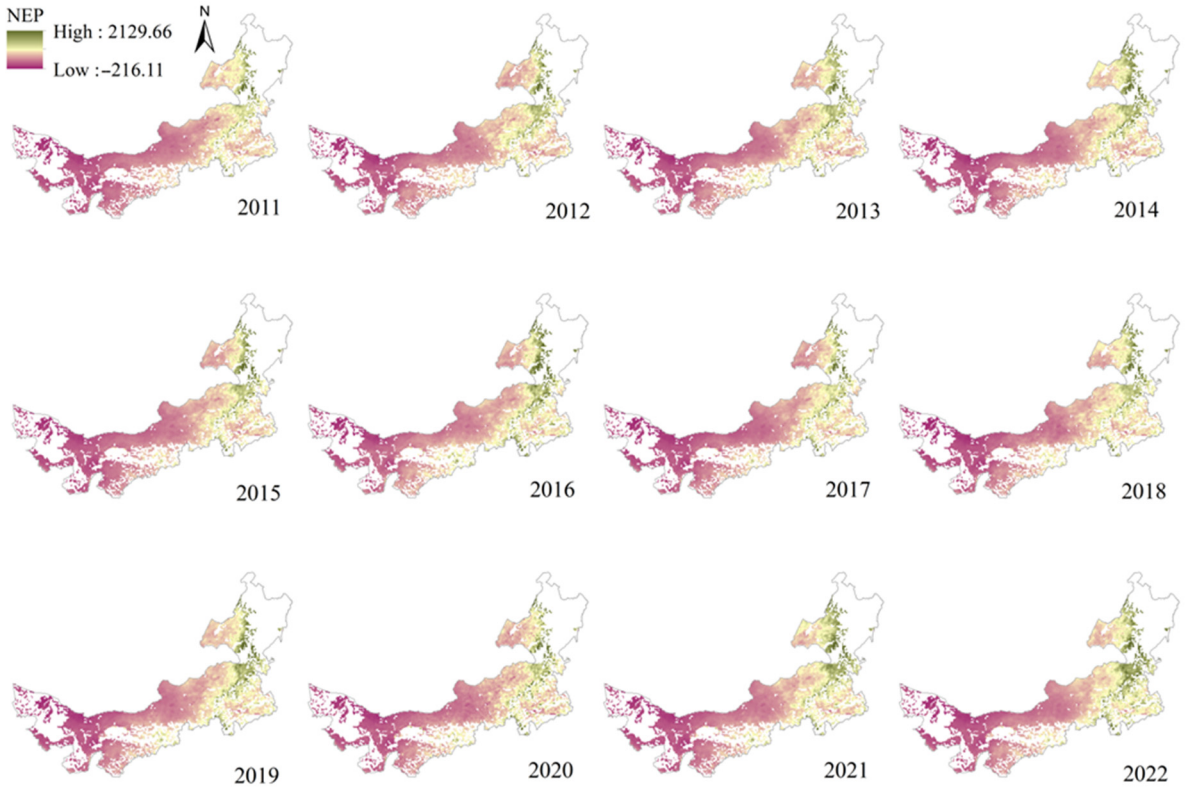


Figure 4. Spatial distribution of the annual average of monthly NEP from 2011 to 2022.

3.2. Temporal Characteristics of NPP and NEP in the Inner Mongolia Grassland Ecosystem

The monthly variations of NPP and NEP from 2011 to 2022 are shown in Figure 5. The changes in both NPP and NEP increased and then decreased in the Inner Mongolia grassland ecosystem, showing a single peak. NPP and NEP were highest in summer and

lowest in winter. NPP had its lowest values of 4.66 gC · m^{-2} · month^{-1} in January. NPP increased gradually from January to April, then quickly from April to July, peaking at NPP 46.54 gC · m^{-2} · month^{-1} in July. Then, from August to October, there was a quick decrease to below-average level, followed by a gradual decline over the next two months. NEP showed a slow upward trend from January to August, with only a slight downward trend in April, reaching a maximum annual NEP of 11.09 gC · m^{-2} · month^{-1} in July. The NEP began to fall sharply from August to November, reaching a low of −1.49 gC · m^{-2} · month^{-1} in October, after which it began to rise slowly again.

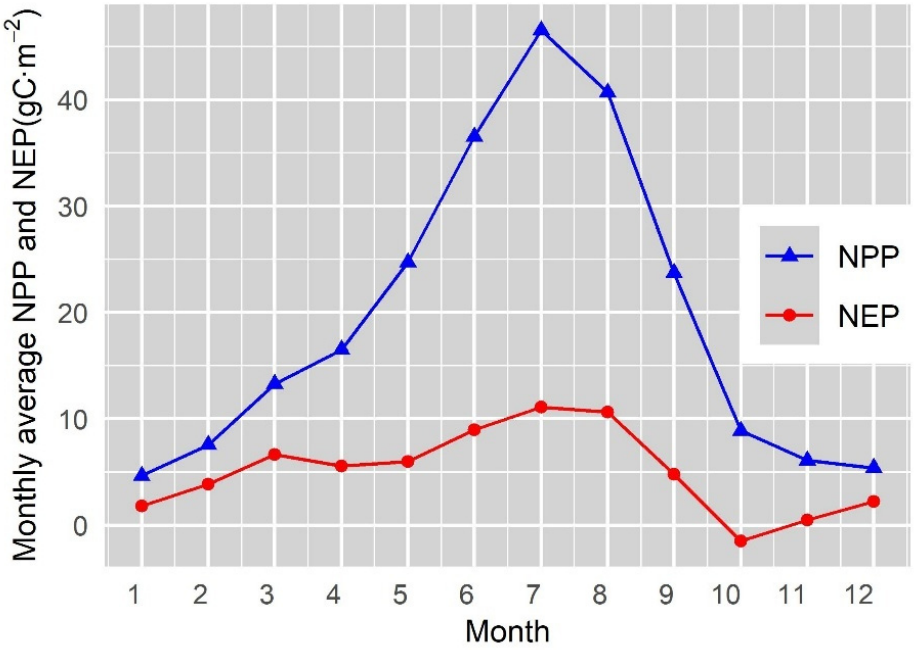


Figure 5. Monthly average analysis results of NPP and NEP in the Inner Mongolia grassland ecosystem from 2011 to 2022.

3.3. Spatial Distribution of NPP and NEP Driving Factors in the Inner Mongolia Grassland Ecosystem

The annual mean spatial distribution of each driving factor from 2011 to 2022 is shown in Figure 6. In Figure 6a, the NDVI values varied between −0.06 and 0.58, with a mean value of 0.20. The areas with larger NDVI values were located in northeastern Inner Mongolia, gradually decreasing from east to west. In Figure 6b, the solar radiation ranged from 3402.85 MJ · m^{-2} to 6601.82 MJ · m^{-2}, with an 11-year average of 4704.78 MJ · m^{-2}. The monthly total solar radiation levels were low in northeastern Inner Mongolia, gradually increasing from east to west, and higher in the west. In Figure 6c, the monthly total precipitation ranged from 13.87 mm to 667.03 mm, with an average value of 4732.43 mm. The regions with the most precipitation were in eastern Inner Mongolia, and mostly overlapped the areas with the highest NDVI values. The precipitation trend was also the same as the NDVI, decreasing from east to west with less precipitation in the west. In Figure 6d, the temperature ranged from −2.68 °C to 11.16 °C, with an 11-year average of 4.72 °C. The temperature was lower in eastern and northern Inner Mongolia, and the trend was consistent with solar radiation, which progressively increased from east to west, with the greatest temperature in western Inner Mongolia.

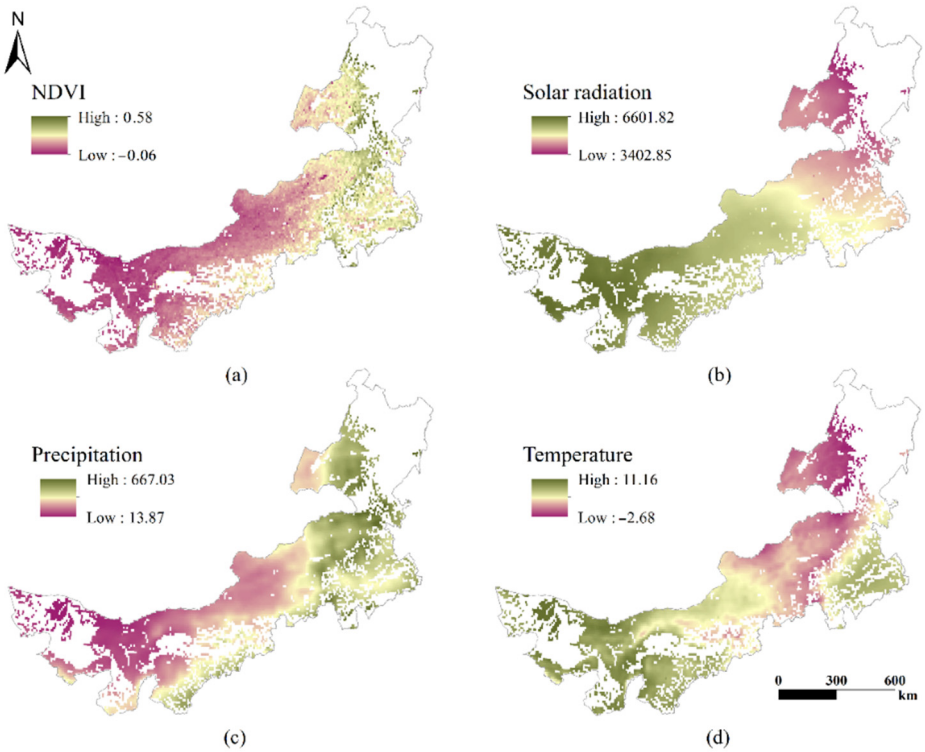


Figure 6. Spatial distribution of the driving factor of NPP and NEP from 2011 to 2022, including NDVI (**a**), Solar radiation (**b**), Precipitation (**c**) and Temperature (**d**).

The interannual differences in temperature were mainly manifested in the central region of Inner Mongolia and the western part of Hulun Buir, and they seemed to have an upward trend. Meanwhile, the remaining regions remained almost unchanged in each year. The spatial characteristics of the entire 12 years from 2011 to 2022 have been retained, as shown in Figure 7. Except for the extremely arid Alxa, all regions have obvious changes in each year, as shown in Figure 8.

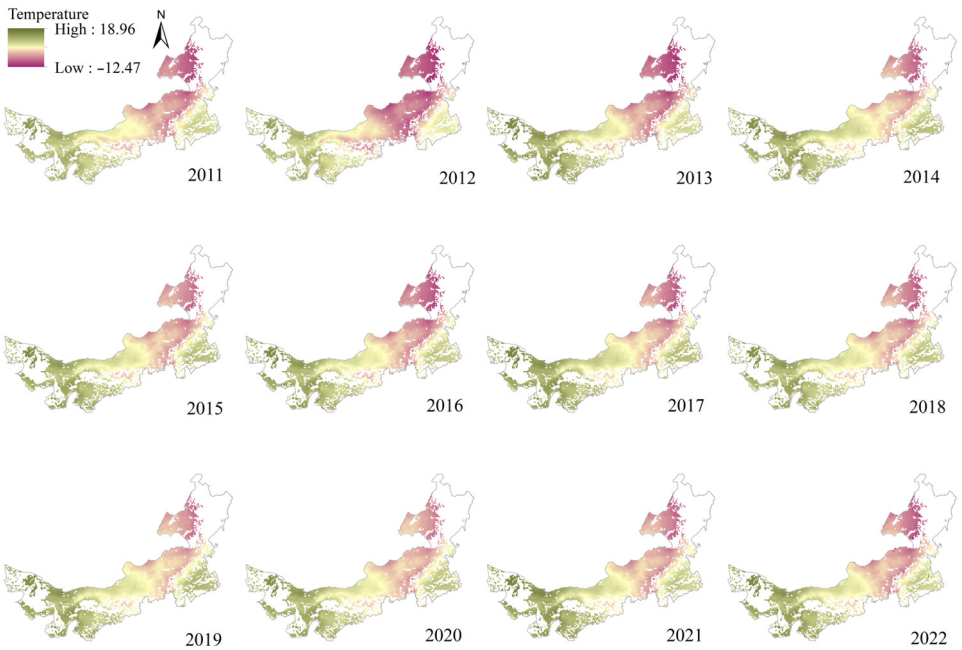


Figure 7. Spatial distribution of the annual average monthly temperature from 2011 to 2022.

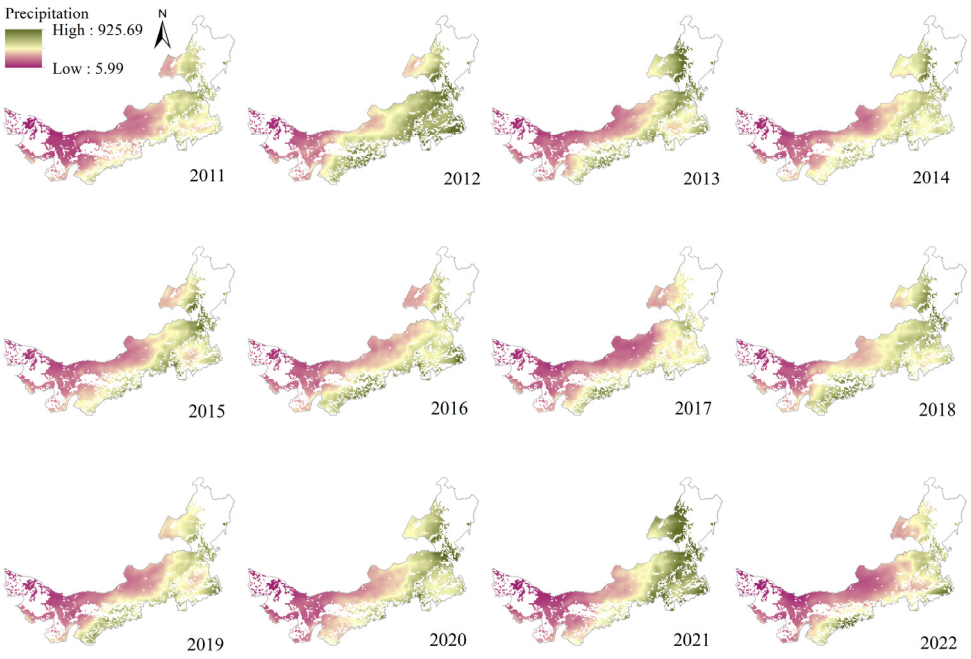


Figure 8. Spatial distribution of the annual total monthly precipitation from 2011 to 2022.

3.4. Temporal Distribution of Temperature and Precipitation in the Inner Mongolia Grassland Ecosystem

The monthly variations of temperature and precipitation from 2011 to 2022 are shown in Figures 9 and 10. The maximum values of temperature and precipitation occur in July (as do those of NPP and NEP), and the value corresponding to the month becomes smaller as the distance from July increases, as does that of NPP.

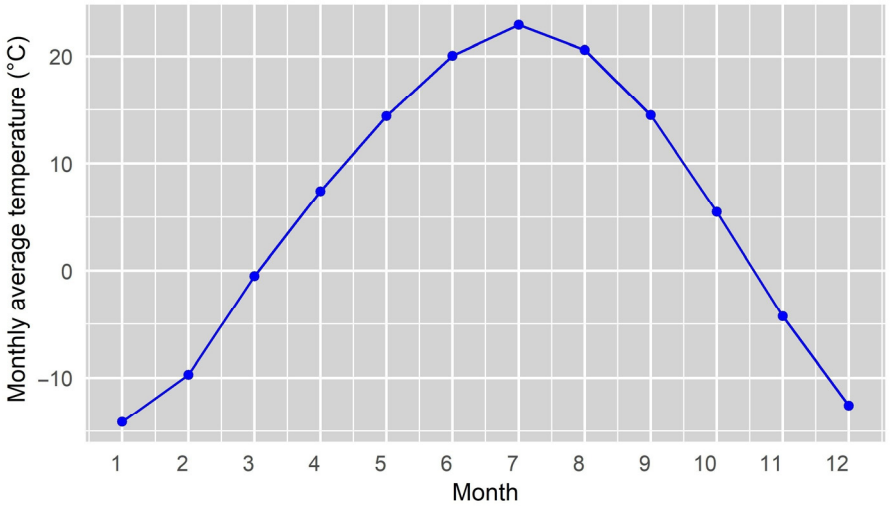


Figure 9. Monthly average analysis results of temperature in the Inner Mongolia grassland ecosystem from 2011 to 2022.

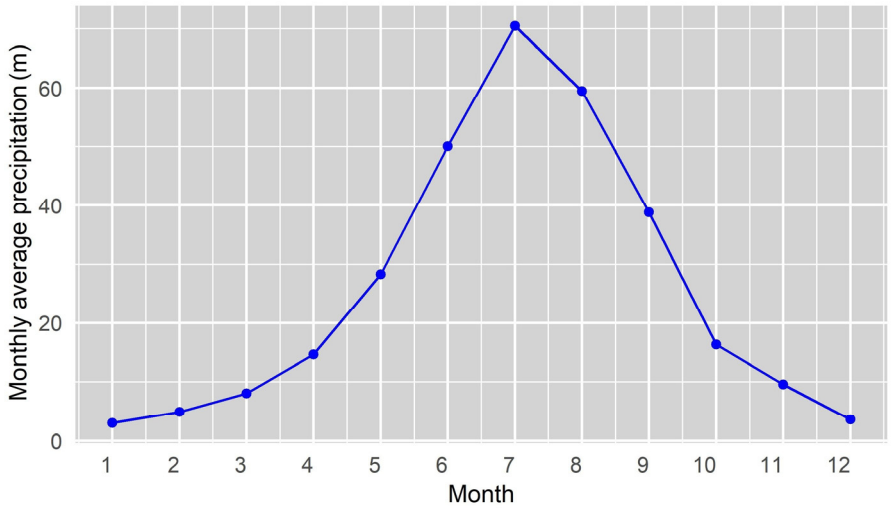


Figure 10. Monthly average analysis results of precipitation in the Inner Mongolia grassland ecosystem from 2011 to 2022.

3.5. Analysis of Factors Influencing Spatial Variation in NPP

Fitting by the MGWR model for NPP, the $R^2 = 0.98$ obtained by fitting the model indicated that the fitting result of this model was good (Table 2), and additional analysis could be carried out.

Table 2. NPP used MGWR bandwidth coefficients and model diagnostic information.

Variable	Bandwidth	Value	t-val (95%)
NDVI	46	0.97	4.20
Solar radiation	157	0.09	3.86
Precipitation	706	0.01	3.33
Temperature	56	−0.07	4.09
$R^2 = 0.98$	AICc = −44,996.39	ENP = 3504.77	RSS = 517.69

Explanation: Bandwidth is the number of surrounding points to be used for local estimation using the MGWR model. AICc is a standard used to measure the goodness of fit of the statistical model. ENP is the effective number of parameters.

Table 2 shows the statistical description of the individual estimated coefficients of the MGWR model for the explanatory and explained factors in the study region. Figure 11 depicts the spatial distribution of the regression coefficients on NPP as influenced by the factors at a significance level of 0.05. Figure 11a shows that the NDVI had a positive effect on NPP, with a significant level of influence. The NDVI regression coefficient had a mean of 0.97, meaning that for every unit increase in NDVI, the NPP average increased by 0.97 $gC \cdot m^{-2}$. As shown in Figure 11b, there was an overall positive correlation between solar radiation and NPP, primarily observed in the eastern region and part of the western region of Inner Mongolia. The mean regression coefficient of solar radiation was 0.09, implying that for every unit increase in solar radiation, the NPP average increased by 0.09 $gC \cdot m^{-2}$. The influence of precipitation on NPP was significantly negatively correlated in most eastern regions of Inner Mongolia, negative in some central regions, and insignificant in other regions. The mean regression coefficient of precipitation was −0.01, which means that for every unit increase in precipitation, the NPP decreased by an average of $-0.01\ gC \cdot m^{-2}$. The effect of temperature on NPP was significantly negative in most areas of eastern Inner Mongolia and significantly positive in southeastern and parts of western Inner Mongolia. The mean value of the temperature regression coefficient was $-0.07\ gC \cdot m^{-2}$, which means that for every 1 unit increase in temperature, the NPP decreased by an average of $-0.07\ gC \cdot m^{-2}$

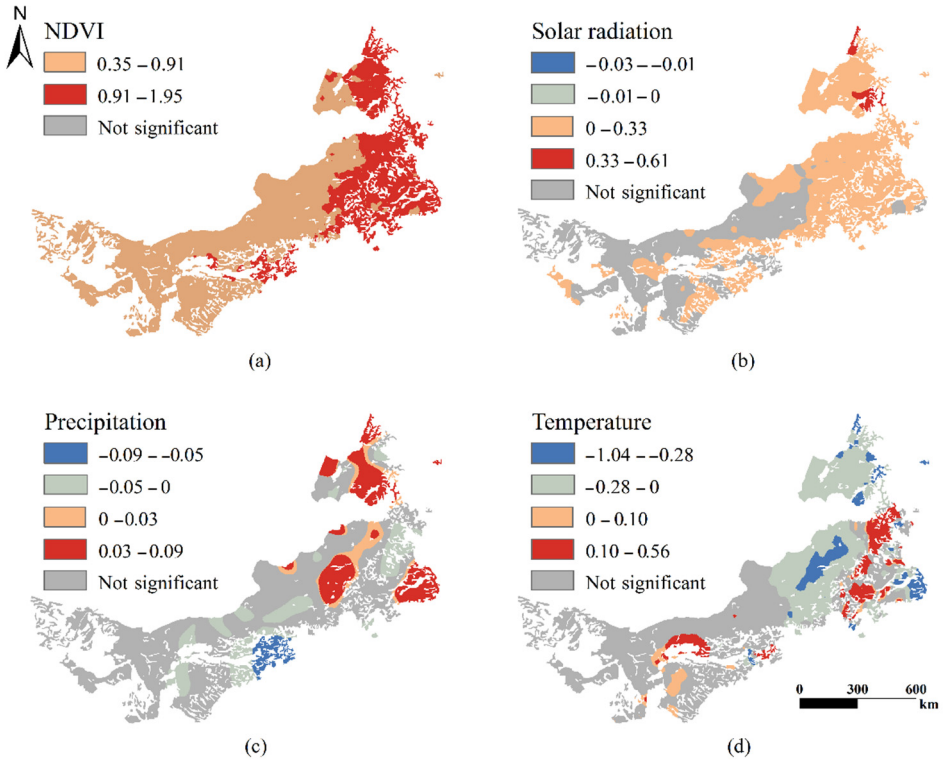


Figure 11. Spatial distribution of estimated coefficients for each of the NPP impact factors (significance level $\alpha = 0.05$), including NDVI (**a**), Solar radiation (**b**), Precipitation (**c**) and Temperature (**d**).

3.6. Analysis of Factors Influencing Spatial Variation in NEP

Fitting by the MGWR model for NEP, the goodness of fit $R^2 = 0.98$ obtained after fitting the model indicated that the model had a good fitting effect (Table 3), and additional research could continue.

Table 3. MGWR bandwidth coefficients used for NEP and model diagnostic information.

Variable	Bandwidth	Mean	t-val (95%)
NDVI	46	0.95	4.20
Solar radiation	157	0.09	3.86
Precipitation	652	−0.08	3.36
Temperature	56	−0.19	4.09
$R^2 = 0.98$	AICc = −46,525.612	ENP = 3517.42	RSS = 496.26

When R_h was calculated, the relationship between NPP and NEP was defined as a basic linear relationship. Hence, the NEP had identical spatial coefficient profiles when fitted with the MGWR model and similar final fits with the same driving variables.

Figure 12 shows the regression coefficients of NEP as impacted by the factors with the MGWR model at a significance level of 0.05. The bandwidth of the NDVI took the same value in the NEP model as in the NPP model (Table 3). It can be seen that the effect of NDVI on NEP was also significantly positively correlated in the whole of Inner Mongolia, just as it was for NPP. The bandwidth value of solar radiation in the NEP model was the same as that of the NPP model, and the distribution of coefficient of the effect on NEP was also similar to NPP. It was significantly positively correlated in northeast Inner Mongolia, and the only difference occurred in western Inner Mongolia, where the effect of solar radiation on NPP was not significant, and it was significantly negatively correlated with NEP. The bandwidth value of precipitation was different in the NEP model than in the NPP model, and the distribution plot of the regression coefficient values also differed significantly. The

effect of precipitation on NEP was significantly negative in most regions of Inner Mongolia. The bandwidth value of temperature was also not the same in the NEP model as in the NPP model, and the distribution of regression coefficients was plotted in a larger region of significant negative correlation compared to the NPP. The effect of temperature on NEP in western Inner Mongolia showed a significant negative correlation.

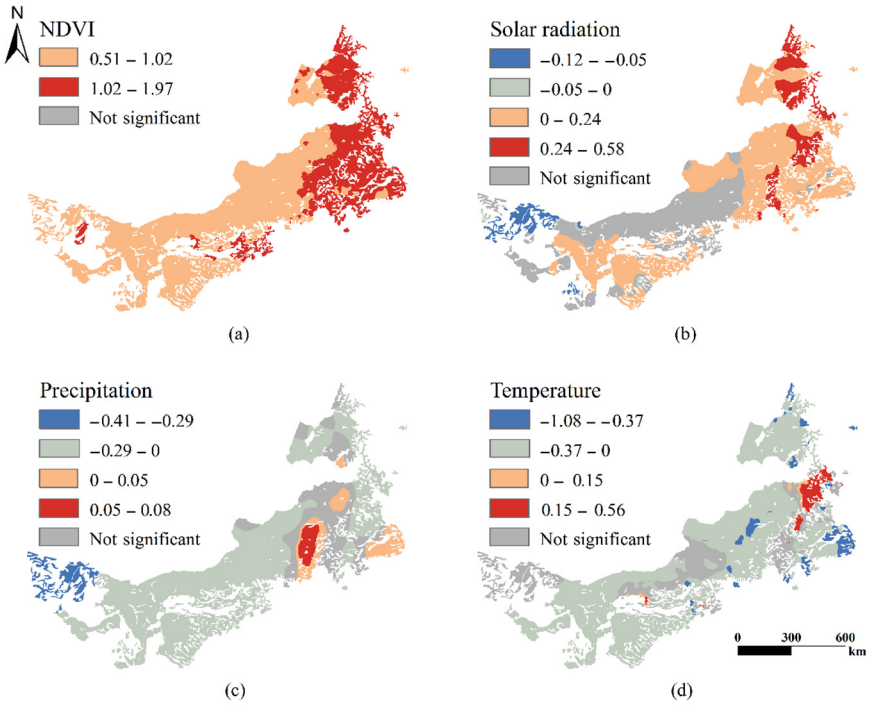


Figure 12. Spatial distribution of estimated coefficients for each of the NEP impact factors (significance level $\alpha = 0.05$), including NDVI (**a**), Solar radiation (**b**), Precipitation (**c**) and Temperature (**d**).

4. Discussion

4.1. Spatiotemporal Patterns of NPP, NEP, and Driving Factors in the Inner Mongolia Grassland Ecosystem

The geographical distribution of NPP and NEP steadily decreased from east to west, with high concentrations in the northeast and low concentrations in the southwest of the Inner Mongolia grassland ecosystem, which was consistent with previous studies [8,33]. The major vegetation type in eastern Inner Mongolia was meadow grassland with high NPP and NEP, while in western Inner Mongolia, the major vegetation cover was desert grassland with low NPP and NEP [8]. NPP and NEP reached maximum values in summer and minimum values in winter [9,13,37]. This was because NPP and NEP were larger in the summer when the herbage entered the growing stage and smaller in the winter when it entered the withering stage [37].

From the perspective of interannual data, the NPP and NEP in the northern part of Xilingol and the western part of Hulun Buir were not as stable as those in other areas, and the changes in the driving factors were not limited to these two areas. This seems to indicate that the grassland ecosystems in these areas were insufficiently stable and were greatly affected by the weather. From the perspective of the monthly variation in the data, NPP and NEP had a positive correlation with temperature and precipitation. In July, they were all at their peak, while in winter, they were at their lowest.

4.2. Spatial Driving Factors of NPP and NEP

The effect of the NDVI on NPP exhibited a substantial positive connection, which was the key influencing factor of NPP in the MGWR model analysis of NPP and NEP in this study. This finding supports the conclusions of some other researchers, who reported that when meteorological factors were selected as influences on NPP and NEP, precipitation was the main factor causing changes in NPP and NEP [38], but when the NDVI was available as a driving factor, the NDVI was usually the most dominant factor. Moreover, they stated that climatic factors influenced NPP and NEP by influencing the NDVI [9,26,39]. The higher the area of vegetation cover, the greater the NDVI value. Hence, maintaining and growing vegetation cover is critical if NPP is to increase. Over the last 20 years, the NDVI has increased dramatically in China, and it has been a crucial contributor to the expansion of the Chinese terrestrial ecosystem carbon sink [37].

Overall, solar radiation and NPP and NEP showed positive correlations, with most of the regions being significantly positively correlated, and only a few negatively correlated. C. Zhang et al. noted the existence of a negative correlation, which could be because stronger solar radiation increased water evaporation, which was not conducive to plant growth, thus causing solar radiation and NPP and NEP to be negatively correlated [40]. It has also been noted that increased evapotranspiration resulting from stronger solar radiation would inhibit vegetation growth by reducing soil moisture, leading to a decrease in NEP [41,42].

Precipitation was positively connected with NPP and NEP in the east–central section of Inner Mongolia and the western part of Hulun Buir. However, semiarid areas in eastern Inner Mongolia and desert areas in western Inner Mongolia showed negative correlations. This situation arose because of insufficient precipitation in these two regions; nevertheless, higher solar radiation and temperatures also featured there. The lack of water supply in the semiarid and arid zones inhibited the utilization of light and heat by plants, resulting in restricted plant growth, which in turn inhibited NPP and NEP from increasing [21]. The coefficient distribution plot for precipitation in NEP had a small positive area of influence, consistent with findings from empirical studies by Noormets [43]. Because of the presence of soil Rh, the results of Rh and NPP regarding soil drought treatments are different, leading to some differences in the responses of NPP and NEP to precipitation and drought. Furthermore, although there was abundant precipitation, there was a negative correlation in some eastern regions. This could be attributed to changes in vegetation growth resulting from the excessive precipitation. As a result, the changes in NPP and NEP were explained by the NDVI, making precipitation a secondary factor that altered the correlation [44].

The overall effect of temperature on NPP and NEP was negative. Previous studies have shown that higher temperatures are usually accompanied by higher evapotranspiration and latent heat of evapotranspiration, resulting in insufficient water availability and inhibition of plant physiological responses [45,46] leading to decreases in NPP and NEP.

Water is a significant limiting element for plant growth and photosynthesis in grassland ecosystems [47]. Nevertheless, the water evaporation rate increases when the temperature rises, exposing plants to more water stress, which can limit NPP and NEP growth [21,48]. Furthermore, in more arid situations, grass cover decreases, growth cycles are shorter, and productivity is lower. The correlation between NPP and NEP and annual climate change could be expressed indirectly through plant biomass and growing season length [45]. This results in the degree of explanation of NPP and NEP by precipitation and temperature being below the threshold of significance in specific areas currently, with the correlation being either nonsignificant or shifting from positive to negative.

However, this study has some limitations. First, the spatial resolution of the original meteorological data used was too large, resulting in certain spatial errors. In subsequent

studies, it will be possible to use data with a smaller spatial resolution. Second, resampling was used to unify spatial resolution, a process that introduces uncertainty. This was due to the fact that it required spatial interpolation of the original data, which may have resulted in inaccuracies or the loss of some locally relevant information. Third, the role of using the spatial variable coefficient model to explain the driving factors may not be as good as that of the spatiotemporal variable coefficient model. More applicable models should be considered to explain the relationship between NPP, NEP, and the driving factors on a monthly basis. Finally, the interpretations of NPP, NEP, and driving factors were all described statistically, while NPP and NEP are ecological concepts related to human activities [49], concentration [50], soil [51,52], etc. Each process should be explained from a more ecological perspective. Further studies on NPP and NEP can be conducted in combination with statistics and ecology.

5. Conclusions

The NPP and NEP in the Inner Mongolia grassland ecosystem from 2011 to 2022 were computed in this study, and the 11-year average value of NPP in the study region was 234.22 $gC \cdot m^{-2} \cdot a^{-1}$, while the value of NEP was 60.31 $gC \cdot m^{-2} \cdot a^{-1}$. Overall, the Inner Mongolian grassland ecosystem was a carbon sink, and the carbon sink sectors were larger than the carbon source sectors, which were mostly in the desert grassland area of western Alxa. The regional distributions of both NPP and NEP decreased from northeast to southwest, indicating that they had spatial heterogeneity. From the perspective of time, NPP and NEP peaked in the summer, and were at a minimum in winter. The monthly average changes in temperature and precipitation reflect their close relationship with this phenomenon. Unlike in other regions, the annual average of monthly NPP and NEP in the northern part of Xilingol and the western part of Hulun Buir were unstable, exposing the vulnerability of these areas.

In this study, the MGWR model was built from a scale perspective to study the relationships between NPP and NEP and their likely drivers in the Inner Mongolia grassland ecosystem. The results showed that the effects of the NDVI and solar radiation on NPP and NEP were positive, the effect of temperature on NPP and NEP was negative, and precipitation had a positive effect on NPP and a negative effect on NEP. Precipitation was the key climatic element, while the NDVI was the dominant factor influencing these four variables. The results revealed the spatial heterogeneity of carbon sources/sinks in the Inner Mongolia grassland ecosystem and the relationship between the driving factors. This information is very important for policy formulation by the relevant management departments of grassland ecosystems.

Author Contributions: Conceptualization, R.W. (Ritu Wu); Methodology, R.W. (Ritu Wu) and Z.H.; Software, R.W. (Ritu Wu), Z.H., W.D., R.W. (Rihan Wu) and Y.S.; Investigation, R.W. (Ritu Wu); Data curation, R.W. (Ritu Wu); Writing—original draft, R.W. (Ritu Wu); Writing—review & editing, R.W. (Ritu Wu), Z.H., W.D., H.Y., R.W. (Rihan Wu), Y.S., S.B. and D.X.; Visualization, R.W. (Rihan Wu); Supervision, Z.H., W.D., H.Y. and Y.S. All authors have read and agreed to the published version of the manuscript.

Funding: This study was supported by multiple funding projects, including the Key Special Project of Inner Mongolia's "Science and Technology for the Development of Mongolia" Action Plan (2020ZD0028), the Inner Mongolia Autonomous Region Science and Technology Program (2024KJHZ0002, 2022YFSH0027, 2024KJHZ0007), the National Natural Science Foundation of China (81860605), the Basic Scientific Research Business Expense Project of Colleges and Universities Directly under Inner Mongolia (JY 20220087), and the Inner Mongolia Natural Science Foundation Project (2023MS01001).

Institutional Review Board Statement: Not applicable.

Informed Consent Statement: Not applicable.

Data Availability Statement: The original contributions presented in this study are included in the article. Further inquiries can be directed to the corresponding author.

Acknowledgments: We are grateful for the fieldwork support from the Arshan Forest and Grassland Disaster Prevention and the Mitigation Field Scientific Observation and Research Station of the Inner Mongolia Autonomous Region.

Conflicts of Interest: The authors declare no conflict of interest.

References

1. Xu, J.; Li, Y.; Hu, F.; Wang, L.; Wang, K.; Ma, W.; Ruan, N.; Jiang, W. Spatio-Temporal Variation of Carbon Emission Intensity and Spatial Heterogeneity of Influencing Factors in the Yangtze River Delta. *Atmosphere* **2023**, *14*, 163. [CrossRef]
2. Piao, S.; Yue, C.; Ding, J.; Guo, Z. Perspectives on the role of terrestrial ecosystems in the 'carbon neutrality' strategy. *Sci. China Earth Sci.* **2022**, *65*, 1178–1186. [CrossRef]
3. Fang, J.; Guo, Z.; Piao, S.; Chen, A. Terrestrial vegetation carbon sinks in China, 1981–2000. *Sci. China Ser. D-Earth Sci.* **2007**, *50*, 1341–1350. [CrossRef]
4. Yang, W.; Zeng, L.; Li, X. Advances in research of carbon sinks and their influencing factors evaluation. *Adv. Earth Sci.* **2023**, *38*, 151–167.
5. IPCC. *Global Warming of 1.5 °C: IPCC Special Report on Impacts of Global Warming of 1.5 °C Above Pre-Industrial Levels in Context of Strengthening Response to Climate Change, Sustainable Development, and Efforts to Eradicate Poverty*, 1st ed.; Cambridge University Press: Cambridge, UK, 2022.
6. Piao, S.; He, Y.; Wang, X.; Chen, F. Estimation of China's terrestrial ecosystem carbon sink: Methods, progress and prospects. *Sci. China Earth Sci.* **2022**, *65*, 641–651. [CrossRef]
7. Gao, S.; Zhao, X.; Fang, J. Carbon Sequestration of Grassland in China. *Strateg. Study CAE* **2016**, *18*, 73–79.
8. Dai, E.; Huang, Y.; Wu, Z.; Zhao, D. Analysis of Spatio-Temporal Features of a Carbon Source/Sink and Its Relationship to Climatic Factors in the Inner Mongolia Grassland Ecosystem. *J. Geogr. Sci.* **2016**, *26*, 297–312. [CrossRef]
9. Zhang, J.; Liu, M.; Zhang, M.; Yang, J.; Cao, R.; Malhi, S.S. Changes of Vegetation Carbon Sequestration in the Tableland of Loess Plateau and Its Influencing Factors. *Environ. Sci. Pollut. Res.* **2019**, *26*, 22160–22172. [CrossRef]
10. Zhao, J.; Yan, X.; Jia, G. Changes in Carbon Budget of Northeast China Forest Ecosystems under Future Climatic Scenario. *Chin. J. Ecol.* **2009**, *28*, 781–787.
11. Rowe, R.L.; Cooper, H.M.; Hastings, A.; Mabey, A.; Keith, A.M.; McNamara, N.P.; Morrison, R. Low risk management intervention: Limited impact of remedial tillage on net ecosystem carbon balance at a commercial Miscanthus plantation. *Glob. Change Biol. Bioenergy* **2024**, *16*, e13114. [CrossRef]
12. Zhang, K.; Zhu, C.; Ma, X.; Zhang, X.; Yang, D.; Shao, Y. Spatiotemporal Variation Characteristics and Dynamic Persistence Analysis of Carbon Sources/Sinks in the Yellow River Basin. *Remote Sens.* **2023**, *15*, 323. [CrossRef]
13. Liang, L.; Geng, D.; Yan, J.; Qiu, S.; Shi, Y.; Wang, S.; Wang, L.; Zhang, L.; Kang, J. Remote Sensing Estimation and Spatiotemporal Pattern Analysis of Terrestrial Net Ecosystem Productivity in China. *Remote Sens.* **2022**, *14*, 1902. [CrossRef]
14. Potter, C.S.; Randerson, J.T.; Field, C.B.; Matson, P.A.; Vitousek, P.M.; Mooney, H.A.; Klooster, S.A. Terrestrial Ecosystem Production: A Process Model Based on Global Satellite and Surface Data. *Glob. Biogeochem. Cycles* **1993**, *7*, 811–841. [CrossRef]
15. Lieth, H.; Whittaker, R.H. *Primary Productivity of the Biosphere*; Springer: Berlin/Heidelberg, Germany, 1975.
16. Yin, C.; Luo, M.; Meng, F.; Sa, C.; Yuan, Z.; Bao, Y. Contributions of Climatic and Anthropogenic Drivers to Net Primary Productivity of Vegetation in the Mongolian Plateau. *Remote Sens.* **2022**, *14*, 3383. [CrossRef]
17. Fang, J.; Ke, J.; Tang, Z.; Chen, A. Implications and Estimations of Four Terrestrial Productive Parameters. *Acta Phytoecol. Sin.* **2001**, *25*, 414–419.
18. Pei, Z.Y.; Ouyang, H.; Zhou, C.-P.; Xu, X.-L. Carbon Balance in an Alpine Steppe in the Qinghai-Tibet Plateau. *J. Integr. Plant Biol.* **2009**, *51*, 521–526. [CrossRef]
19. Zhang, J.; Hao, X.; Hao, H.; Fan, X.; Li, Y. Climate Change Decreased Net Ecosystem Productivity in the Arid Region of Central Asia. *Remote Sens.* **2021**, *13*, 4449. [CrossRef]
20. Li, Z.; Shan, N.; Wang, Q.; Li, W.; Wang, Z.; Bao, S.; Dou, H.; Ao, W.; Pang, B.; Wang, W. Estimation of Vegetation Carbon Source/Sink and Analysis of Its Influencing Factors in Hulun Lake Basin from 2013 to 2020. *J. Ecol. Rural Environ.* **2022**, *38*, 1437–1446.
21. Wu, L.; Ma, X.; Dou, X.; Zhu, J.; Zhao, C. Impacts of Climate Change on Vegetation Phenology and Net Primary Productivity in Arid Central Asia. *Sci. Total Environ.* **2021**, *796*, 149055. [CrossRef]

22. Ge, W.; Deng, L.; Wang, F.; Han, J. Quantifying the Contributions of Human Activities and Climate Change to Vegetation Net Primary Productivity Dynamics in China from 2001 to 2016. *Sci. Total Environ.* **2021**, *773*, 145648. [CrossRef]
23. Xu, J. Estimation of the spatial distribution of potential forestation land and its climatic potential productivity in China. *Acta Geogr. Sinica.* **2023**, *78*, 677–693.
24. Liu, C.; Dong, X.; Wang, C.; Ding, R. Time and space variability of the county level administrative unit to NEP Gansu Province. *J. Lanzhou Univ. Nat. Sci.* **2018**, *54*, 82–89.
25. Zhang, Z.; Xiong, M.; Li, F.; Liu, X.; Hao, Y.; Xing, L.; Wang, X.; Lai, M.; Yuan, P. Analysis of the temporal and spatial variations in net primary productivity of in the grassland region of Inner Mongolia and the factors influencing those changes. *Pratac. Sci.* **2022**, *39*, 2492–2502.
26. Song, L.; Li, M.; Xu, H.; Guo, Y.; Wang, Z.; Li, Y.; Wu, X.; Feng, L.; Chen, J.; Lu, X.; et al. Spatiotemporal Variation and Driving Factors of Vegetation Net Primary Productivity in a Typical Karst Area in China from 2000 to 2010. *Ecol. Indic.* **2021**, *132*, 108280. [CrossRef]
27. Shen, T.; Yu, H.; Zhou, L.; Gu, H.; He, H. On Hedonic Price of Second-Hand Houses in Beijing Based on Multi-Scale Geographically Weighted Regression: Scale Law of Spatial Heterogeneity. *Econ. Geogr.* **2020**, *40*, 75–83.
28. Lu, B.; Ge, Y.; Shi, Y.; Zheng, J.; Harris, P. Uncovering Drivers of Community-Level House Price Dynamics through Multiscale Geographically Weighted Regression: A Case Study of Wuhan, China. *Spat. Stat.* **2023**, *53*, 100723. [CrossRef]
29. Nazia, N.; Law, J.; Butt, Z.A. Spatiotemporal Clusters and the Socioeconomic Determinants of COVID-19 in Toronto Neighbourhoods, Canada. *Spat. Spatio-Temporal Epidemiol.* **2022**, *43*, 100534. [CrossRef]
30. Oshan, T.M.; Smith, J.P.; Fotheringham, A.S. Targeting the Spatial Context of Obesity Determinants via Multiscale Geographically Weighted Regression. *Int. J. Health Geogr.* **2020**, *19*, 11. [CrossRef]
31. Fotheringham, A.S.; Yang, W.; Kang, W. Multiscale Geographically Weighted Regression (MGWR). *Ann. Am. Assoc. Geogr.* **2017**, *107*, 1247–1265. [CrossRef]
32. Wu, N.; Liu, G.; Yang, Y.; Song, X.; Bai, H. Dynamic monitoring of net primary productivity and its response to climate factors in native grassland in Inner Mongolia using a light-use efficiency model. *Acta Prataculturae Sin.* **2020**, *29*, 1–10.
33. Huang, L.; Zhou, W.; Li, J.; Wen, W. Analysis on spatial-temporal dynamics of different types grassland NPP and its climate influencing factors in Inner Mongolia. *Grassl. Turf* **2019**, *39*, 1–9.
34. Muñoz-Sabater, J.; Dutra, E.; Agustí-Panareda, A.; Albergel, C.; Arduini, G.; Balsamo, G.; Boussetta, S.; Choulga, M.; Harrigan, S.; Hersbach, H.; et al. ERA5-Land: A State-of-the-Art Global Reanalysis Dataset for Land Applications. *Earth Syst. Sci. Data* **2021**, *13*, 4349–4383. [CrossRef]
35. Zhu, W.; Pan, Y.; Zhang, J. Estimation of net primary productivity of Chinese terrestrial vegetation based on remote sensing. *J. Plant Ecol.* **2007**, *31*, 413–424.
36. Zhou, G.S.; Zhang, X.S. Study on climate-vegetation classification for global change in China. *Acta Bot. Sin.* **1996**, *38*, 8–17.
37. Zhou, W.; Huang, L.; Yang, H.; Ju, W.; Yue, T. Interannual Variation in Grassland Net Ecosystem Productivity and Its Coupling Relation to Climatic Factors in China. *Environ. Geochem. Health* **2019**, *41*, 1583–1597. [CrossRef] [PubMed]
38. Zhang, L.; Ren, X.; Wang, J.; He, H.; Wang, S.; Wang, M.; Piao, S.; Yan, H.; Ju, W.; Gu, F.; et al. Interannual Variability of Terrestrial Net Ecosystem Productivity over China: Regional Contributions and Climate Attribution. *Environ. Res. Lett.* **2019**, *14*, 014003. [CrossRef]
39. Huang, Y.; Wang, F.; Zhang, L.; Zhao, J.; Zheng, H.; Zhang, F.; Wang, N.; Gu, J.; Zhao, Y.; Zhang, W. Changes and Net Ecosystem Productivity of Terrestrial Ecosystems and Their Influencing Factors in China from 2000 to 2019. *Front. Plant Sci.* **2023**, *14*, 1120064. [CrossRef]
40. Zhang, Z.; Cai, H.; Zhang, P.; Wang, Z.; Li, T. A GEE-based study on the temporal and spatial variations in the carbon source/sink function of vegetation in the Three-River Headwaters region. *Remote Sens. Nat. Resour.* **2023**, *35*, 231–242.
41. Gao, M.; Xu, R.; Huang, J.; Su, B.; Jiang, S.; Shi, P.; Yang, H.; Xing, Y.; Wang, D.; Jiang, H.; et al. Increase of Carbon Storage in the Qinghai-Tibet Plateau: Perspective from Land-Use Change under Global Warming. *J. Clean. Prod.* **2023**, *414*, 137540. [CrossRef]
42. Hou, Q.; Yang, H.; Wu, J.; Yu, X. Carbon Budget Response to Climate Change Varies with Grassland Type in Qilian Mountains, China. *Glob. Ecol. Conserv.* **2023**, *47*, e02670. [CrossRef]
43. Zhu, Z.; Piao, S.; Myneni, R.B.; Huang, M.; Zeng, Z.; Canadell, J.G.; Ciais, P.; Sitch, S.; Friedlingstein, P.; Arneth, A.; et al. Greening of the Earth and Its Drivers. *Nat. Clim. Chang.* **2016**, *6*, 791–795. [CrossRef]
44. Noormets, A.; Bracho, R.; Ward, E.; Seiler, J.; Strahm, B.; Lin, W.; McElligott, K.; Domec, J.-C.; Gonzalez-Benecke, C.; Jokela, E.J.; et al. Heterotrophic Respiration and the Divergence of Productivity and Carbon Sequestration. *Geophys. Res. Lett.* **2021**, *48*, e2020GL092366. [CrossRef]
45. Michaletz, S.T.; Cheng, D.; Kerkhoff, A.J.; Enquist, B.J. Convergence of Terrestrial Plant Production across Global Climate Gradients. *Nature* **2014**, *512*, 39–43. [CrossRef]
46. Enquist, B.J.; Kerkhoff, A.J.; Huxman, T.E.; Economo, E.P. Adaptive Differences in Plant Physiology and Ecosystem Paradoxes: Insights from Metabolic Scaling Theory. *Glob. Change Biol.* **2007**, *13*, 591–609. [CrossRef]

47. Yuan, M.; Zhu, Q.; Zhang, J.; Liu, J.; Chen, H.; Peng, C.; Li, P.; Li, M.; Wang, M.; Zhao, P. Global Response of Terrestrial Gross Primary Productivity to Climate Extremes. *Sci. Total Environ.* **2021**, *750*, 142337. [CrossRef]
48. Sawut, R.; Li, Y.; Kasimu, A.; Ablat, X. Examining the Spatially Varying Effects of Climatic and Environmental Pollution Fac-tors on the NDVI Based on Their Spatially Heterogeneous Relationships in Bohai Rim, China. *J. Hydrol.* **2023**, *617*, 128815. [CrossRef]
49. Yin, L.; Dai, E.; Zheng, D.; Wang, Y.; Ma, L.; Tong, M. What Drives the Vegetation Dynamics in the Hengduan Mountain Region, Southwest China: Climate Change or Human Activity? *Ecol. Indic.* **2020**, *112*, 106013. [CrossRef]
50. Prăvălie, R.; Niculiță, M.; Roșca, B.; Marin, G.; Dumitrașcu, M.; Patriche, C.; Birsan, M.-V.; Nita, I.A.; Tișcovschi, A.; Sîrodoev, I.; et al. Machine Learning-Based Prediction and Assessment of Recent Dynamics of Forest Net Primary Productivity in Ro-mania. *J. Environ. Manag.* **2023**, *334*, 117513. [CrossRef]
51. Bradford, M.A.; Jones, T.H.; Bardgett, R.D.; Black, H.I.J.; Boag, B.; Bonkowski, M.; Cook, R.; Eggers, T.; Gange, A.C.; Grayston, S.J.; et al. Impacts of Soil Faunal Community Composition on Model Grassland Ecosystems. *Science* **2002**, *298*, 615–618. [CrossRef]
52. Hong, S.; Ding, J.; Kan, F.; Xu, H.; Chen, S.; Yao, Y.; Piao, S. Asymmetry of Carbon Sequestrations by Plant and Soil after Forestation Regulated by Soil Nitrogen. *Nat. Commun.* **2023**, *14*, 3196. [CrossRef]

Disclaimer/Publisher's Note: The statements, opinions and data contained in all publications are solely those of the individual author(s) and contributor(s) and not of MDPI and/or the editor(s). MDPI and/or the editor(s) disclaim responsibility for any injury to people or property resulting from any ideas, methods, instructions or products referred to in the content.